

## Catalytic Activity of Zirconium Oxynitride Prepared by Reactive Sputtering for ORR in Sulfuric Acid

To cite this article: Youta Maekawa *et al* 2008 *Electrochem. Solid-State Lett.* **11** B109

View the [article online](#) for updates and enhancements.



## Catalytic Activity of Zirconium Oxynitride Prepared by Reactive Sputtering for ORR in Sulfuric Acid

Youta Maekawa, Akimitsu Ishihara,\* Jin-Hwan Kim, Shigenori Mitsushima,\* and Ken-ichiro Ota\*<sup>z</sup>

Chemical Energy Laboratory, Yokohama National University, Yokohama, Kanagawa 240-8501, Japan

Zirconium oxynitride ( $\text{ZrO}_x\text{N}_y$ ) prepared by the reactive sputtering method under  $\text{O}_2$  and  $\text{N}_2$  atmosphere was evaluated as a nonplatinum cathode catalyst for polymer electrolyte fuel cells. The  $\text{ZrO}_x\text{N}_y$  prepared at  $p_{\text{Ar}} = 0.886$  Pa,  $p_{\text{N}_2} = 0.41$  Pa, and  $p_{\text{O}_2} = 1.7$  mPa with a substrate temperature of  $800^\circ\text{C}$  during the film formation had a superior catalytic activity for the oxygen reduction reaction (ORR) in sulfuric acid. The onset potential for the ORR had a maximum of  $0.8$  V vs a reversible hydrogen electrode. The thin-film X-ray diffraction analysis and ionization potential measurement revealed that the  $\text{ZrO}_x\text{N}_y$  with a high catalytic activity for the ORR contained the  $\text{Zr}_2\text{ON}_2$  crystalline structure.

© 2008 The Electrochemical Society. [DOI: 10.1149/1.2916441] All rights reserved.

Manuscript submitted January 24, 2008; revised manuscript received April 2, 2008. Available electronically April 28, 2008.

Polymer electrolyte fuel cells (PEFCs) are expected as power sources for residential cogeneration systems and transportation applications due to their high theoretical energy efficiency and lower emission of pollutants. However, PEFCs have some serious problems to be solved before their commercialization. In particular, a large overpotential of the oxygen reduction reaction (ORR) must be reduced in order to obtain a higher energy efficiency. A large amount of platinum is generally used as a cathode catalyst in present PEFCs to decrease the overpotential of the ORR. However, Pt is expensive and its resources are limited, so that Pt usage will be limited for future commercialization of PEFCs. Many methods have been studied to reduce use of the Pt catalyst, such as a greater dispersion of Pt particles and/or alloying with transition metals.<sup>1,2</sup> However, because the dissolution and deposition of highly dispersed Pt particles proceeds during long-term operation,<sup>3</sup> a drastic reduction of Pt usage would be difficult. Therefore, development of a new nonplatinum catalyst is strongly recommended.

We have examined the applicability of transition metal oxynitrides to the cathode catalysts.<sup>4-6</sup> In particular, zirconium oxynitride films prepared using the reactive sputtering method had a definite catalytic activity for the ORR. In addition, as the heating temperature of a substrate during the sputtering increased to  $800^\circ\text{C}$ , the catalytic activity for the ORR increased.<sup>4</sup> In this study, the dependence of the catalytic activity of  $\text{ZrO}_x\text{N}_y$  prepared by reactive sputtering at  $800^\circ\text{C}$  for the ORR on the gas atmosphere during the sputtering was investigated.

### Experimental

Thin-film specimens were prepared using reactive sputtering and were expressed as  $\text{ZrO}_x\text{N}_y$  in this study. The  $\text{ZrO}_x\text{N}_y$  thin films were prepared on the surface of a substrate (a polished glassy carbon rod with  $\phi = 5.2$  mm, Tokai Carbon) with radio frequency magnetron sputtering (MUE-ECO-EV, Ulvac). The metal Zr (99.9%, Furuchi Chemical) was used as a target. The chamber was evacuated to less than  $1.0 \times 10^{-3}$  Pa, and then argon, oxygen, and nitrogen gases were introduced. The  $\text{N}_2$  flow rate was changed from 0 to  $29 \text{ cm}^3 \text{ min}^{-1}$ , and the  $\text{O}_2$  flow rate was changed from 0.01 to  $0.30 \text{ cm}^3 \text{ min}^{-1}$ . The Ar flow was balanced and the total gas flow rate was  $29 \text{ cm}^3 \text{ min}^{-1}$ . The heating temperature of the substrate was always kept at a constant temperature of  $800^\circ\text{C}$  during sputtering. Partial pressures of  $\text{N}_2$  ( $p_{\text{N}_2}$ ) and  $\text{O}_2$  ( $p_{\text{O}_2}$ ) were calculated by multiplying the ratio of the flow rate of each gas and the total pressure in the chamber. A sputtering power and a sputtering time were fixed at 150 W and 80 min, respectively.

The electrochemical measurements were carried out using a three-electrode cell at  $30^\circ\text{C}$  in  $0.1 \text{ M H}_2\text{SO}_4$ . A reversible hydrogen

electrode (RHE) and a carbon plate were used as a reference and a counter electrode, respectively. The electrode potential was referred to the RHE in the present study. In order to evaluate the catalytic activity for the ORR, a slow scan voltammetry (SSV) was performed under  $\text{N}_2$  and  $\text{O}_2$  atmospheres. The scan rate and the potential range of the SSV were  $5 \text{ mV s}^{-1}$  and  $0.2$ – $1.0$  V. Current density was based on the geometric surface area of the working electrode. The current difference between  $\text{O}_2$  and  $\text{N}_2$  corresponds to the oxygen reduction current ( $i_{\text{ORR}}$ ). The electrode potential at the current density of the ORR of  $-0.2 \mu\text{A cm}^{-2}$  was defined as an onset potential of the ORR,  $E_{\text{ORR}}$  (Fig. 1), to evaluate the catalytic activity. Slow scan cyclic voltammetry was also performed under a  $\text{N}_2$  atmosphere to examine the electrochemical stability of the electrode. The scan rate and potential range were  $5 \text{ mV s}^{-1}$  and  $0.2$ – $1.0$  V, respectively.

The thickness of the films was determined by the cross-sectional transmission electron microscopy (TEM) images of the films. The cross-sectional TEM images revealed that the film thickness was ca. 70 nm. Therefore, the crystalline structure was analyzed using thin-film X-ray diffraction (XRD; X'Pert PRD MRD, PANalytical). The angle of the X-ray incidence was kept constant at  $0.40^\circ$ . The chemical composition of  $\text{ZrO}_x\text{N}_y$  was analyzed using Rutherford backscattering spectrometry (RBS; 1 MV Tandem Accelerator, NEC Corp.). The ionization potential was measured using a photoelectron spectroscopic analyzer (AC-2, Riken Keiki).

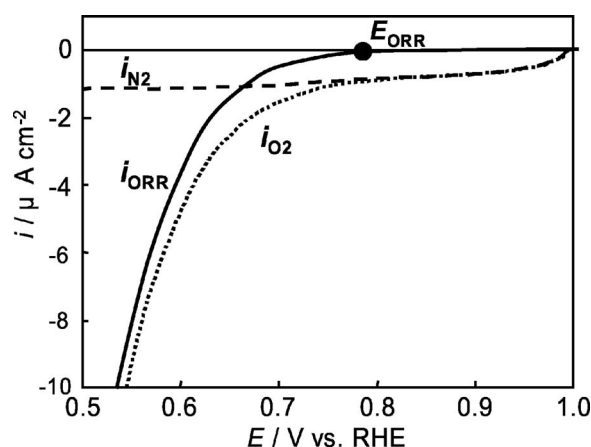


**Figure 1.** SSVs of  $\text{ZrO}_x\text{N}_y$  under a  $\text{N}_2$  ( $i_{\text{N}_2}$ ) or  $\text{O}_2$  ( $i_{\text{O}_2}$ ) atmosphere and the potential vs ORR current ( $i_{\text{ORR}}$ ) curve in  $0.1 \text{ M H}_2\text{SO}_4$  at  $30^\circ\text{C}$  with a scan rate of  $5 \text{ mV s}^{-1}$ .

\* Electrochemical Society Active Member.

<sup>z</sup> E-mail: ken-ota@ynu.ac.jp

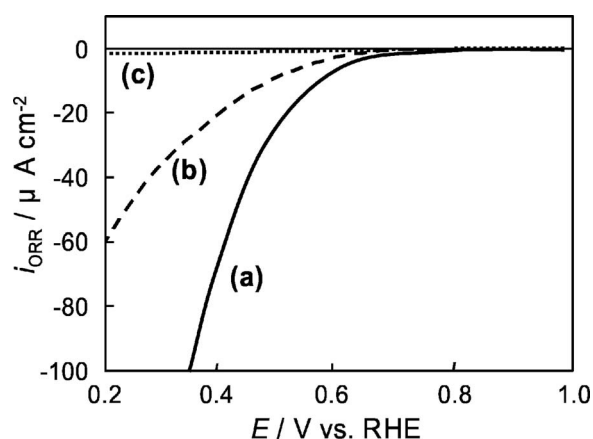


**Figure 2.** Potential vs  $i_{\text{ORR}}$  curves of the  $\text{ZrO}_x\text{N}_y$  prepared under different  $p_{\text{N}_2}$  and  $p_{\text{O}_2}$  in 0.1 M  $\text{H}_2\text{SO}_4$  at  $30^\circ\text{C}$  with a scan rate of  $5 \text{ mV s}^{-1}$ : (a)  $p_{\text{N}_2}/p_{\text{O}_2} = 240$ , (b)  $p_{\text{N}_2}/p_{\text{O}_2} = 2400$ , and (c)  $p_{\text{N}_2}/p_{\text{O}_2} = 0$ .

### Results and Discussion

Figure 2 shows the potential  $i_{\text{ORR}}$  curves of  $\text{ZrO}_x\text{N}_y$  prepared under different  $p_{\text{N}_2}$  and  $p_{\text{O}_2}$ . As shown in Fig. 2a, when the  $\text{N}_2$  and  $\text{O}_2$  flow rates were 24 and  $0.1 \text{ cm}^3 \text{ min}^{-1}$ , ( $p_{\text{Ar}} = 0.086 \text{ Pa}$ ,  $p_{\text{N}_2} = 0.41 \text{ Pa}$ ,  $p_{\text{O}_2} = 1.7 \text{ mPa}$ ), where the gas ratio was  $p_{\text{N}_2}/p_{\text{O}_2} = 240$ . The  $i_{\text{ORR}}$  was started at ca. 0.8 V, indicating that the  $\text{ZrO}_x\text{N}_y$  prepared under  $p_{\text{N}_2}/p_{\text{O}_2} = 240$  had a high catalytic activity for ORR. When the  $\text{O}_2$  flow rate was one-tenth of that at (a), that is,  $p_{\text{N}_2}/p_{\text{O}_2} = 2400$ , the catalytic activity was slightly lower, as shown in Fig. 2b. The  $i_{\text{ORR}}$  of the  $\text{ZrO}_x\text{N}_y$  prepared under Ar +  $\text{O}_2$  without  $\text{N}_2$ , namely,  $p_{\text{N}_2}/p_{\text{O}_2} = 0$ , hardly showed the ORR activity as shown in Fig. 2c. The results indicated that the catalytic activity of  $\text{ZrO}_x\text{N}_y$  for the ORR significantly depended on the gas atmosphere during the sputtering, and the presence of  $\text{N}_2$  in the atmosphere is very important for the ORR activity.

Following these results, the relationship between the catalytic activity for the ORR and  $p_{\text{N}_2}$  or  $p_{\text{O}_2}$  during the sputtering was investigated. Figure 3a shows the relationship between the onset potential ( $E_{\text{ORR}}$ ) and the  $\text{O}_2$  partial pressure during sputtering with an  $\text{N}_2$  flow rate of 10, 24, and  $29 \text{ cm}^3 \text{ min}^{-1}$ . The  $E_{\text{ORR}}$  had a maximum of ca. 0.78 V at approximately 2 mPa of  $p_{\text{O}_2}$ . Therefore, the existence of a moderate amount of  $\text{O}_2$  during the film formation was essential to enhance the catalytic activity for the ORR. Figure 3b shows the relationship between  $E_{\text{ORR}}$  and  $\text{N}_2$  partial pressure during sputtering with an  $\text{O}_2$  flow rate from 0.01 to  $0.30 \text{ cm}^3 \text{ min}^{-1}$ . The  $E_{\text{ORR}}$  value in this figure was saturated at ca. 0.7 V above 0.2 Pa of  $p_{\text{N}_2}$ . In contrast, when no  $\text{N}_2$  was introduced in the chamber, the  $E_{\text{ORR}}$  was 0.2–0.5 V, indicating that the  $\text{ZrO}_x\text{N}_y$  prepared under no  $\text{N}_2$  had a poor catalytic activity. The existence of  $\text{N}_2$  during the sputtering was required to increase the catalytic activity, and the  $p_{\text{N}_2}$  above 0.2 Pa slightly affected the catalytic activity for the ORR. Thus, the  $\text{ZrO}_x\text{N}_y$  thin films, which were prepared by reactive sputtering under  $\text{N}_2$  and a moderate  $\text{O}_2$  atmosphere, have high catalytic activities for the ORR. These results imply that both the nitridation and oxidation of Zr are necessary to produce the catalytic activity for ORR. However, the  $E_{\text{ORR}}$  of the platinum-supported carbon catalyst was ca. 1.05 V. The catalytic activity of the  $\text{ZrO}_x\text{N}_y$  films for the ORR was insufficient. Therefore, the catalytic activity of the  $\text{ZrO}_x\text{N}_y$  films should be enhanced by optimization of the catalyst design.

Figures 4a–c show the thin-film XRD patterns of  $\text{ZrO}_x\text{N}_y$  films prepared under conditions corresponding to Fig. 2a–c, respectively. As shown in Fig. 4a, the  $\text{ZrO}_x\text{N}_y$  with the highest catalytic activity among all specimens prepared under these experimental conditions showed the crystal structure of  $\text{Zr}_2\text{ON}_2$  (JCPDS 50–1170). This result indicated that at a flow ratio of  $p_{\text{N}_2}/p_{\text{O}_2} = 240$ , the nitridation as

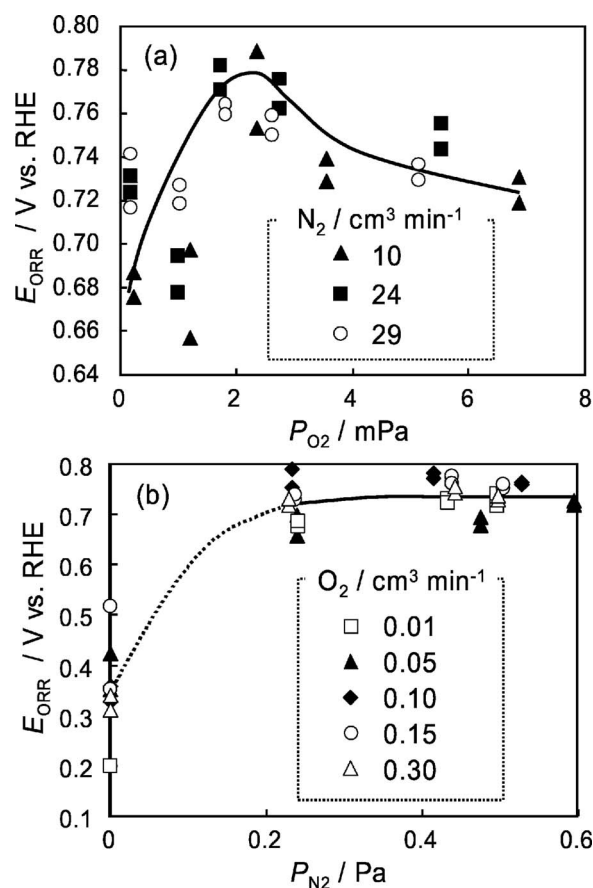


**Figure 3.** Relationships between the  $E_{\text{ORR}}$  and (a)  $p_{\text{O}_2}$  or (b)  $p_{\text{N}_2}$  in 0.1 M  $\text{H}_2\text{SO}_4$  at  $30^\circ\text{C}$ . Scan rate  $5 \text{ mV s}^{-1}$ .

well as the oxidation of Zr took place to form  $\text{Zr}_2\text{ON}_2$ . The  $\text{ZrO}_x\text{N}_y$  with a slightly lower ORR activity, which was prepared at  $p_{\text{N}_2}/p_{\text{O}_2} = 2400$ , had  $\text{ZrN}$  (JCPDS 35–0753) and  $\text{Zr}_7\text{O}_8\text{N}_4$  (JCPDS 50–1172) structures as shown in Fig. 4b. The ratio  $p_{\text{N}_2}/p_{\text{O}_2}$  was 10 times larger; therefore, the nitridation proceeded more than the oxidation to form  $\text{ZrN}$ . However,  $\text{O}_2$  is so much more active than  $\text{N}_2$  that the oxynitride,  $\text{Zr}_7\text{O}_8\text{N}_4$ , formed as well as  $\text{ZrN}$ . Liu et al. prepared the  $\text{ZrO}_x\text{N}_y/\text{C}$  powder by the ammonolysis of carbon-supported zirconia at  $950^\circ\text{C}$ . They revealed that the  $\text{ZrO}_x\text{N}_y/\text{C}$  consisted of the  $\beta$ -phase  $\text{Zr}_7\text{O}_8\text{N}_4$ , and the monoclinic phase  $\text{ZrO}_2$  had a definite catalytic activity for the ORR.<sup>7</sup> However, our results suggested that the  $\text{ZrO}_x\text{N}_y$  having a  $\text{Zr}_2\text{ON}_2$  structure on the surface had a higher catalytic activity for the ORR than that having a  $\text{Zr}_7\text{O}_8\text{N}_4$  structure. As shown in Fig. 4c, when no  $\text{N}_2$  gas was included in the sputtering atmosphere, i.e.,  $p_{\text{N}_2}/p_{\text{O}_2} = 0$ , two kinds of peaks were observed. One was identified as  $\text{ZrO}$  (JCPDS 20–0684), and another peak lay between the peaks of metallic Zr (JCPDS 05–0665) and  $\text{ZrO}_{0.35}$  (JCPDS 17–0385). This pattern indicated that the supply of  $\text{O}_2$  was not enough to form the Zr oxide, although  $\text{O}_2$  was included in the sputtering atmosphere. Following the catalytic activity shown in Fig. 2c, both the metallic Zr,  $\text{ZrO}$ , and  $\text{ZrO}_{0.35}$  had poor catalytic activities for ORR. Thus, we found that the  $\text{ZrO}_x\text{N}_y$  with  $\text{Zr}_2\text{ON}_2$  crystalline structures, which were prepared under  $\text{N}_2$  and moderate  $\text{O}_2$  atmosphere, had a superior catalytic activity for ORR.

RBS analysis was performed to confirm the formation of  $\text{Zr}_2\text{ON}_2$ . The Zr, O, and N atomic percentages of the  $\text{ZrO}_x\text{N}_y$ , which were identified as  $\text{Zr}_2\text{ON}_2$  by the thin-film XRD, were 36, 25, and 39, respectively. These percentages are close to the theoretical values of  $\text{Zr}_2\text{ON}_2$  where the percentages of Zr, O, and N are 40, 20, and 40, respectively. The crystallization of the film was incomplete;

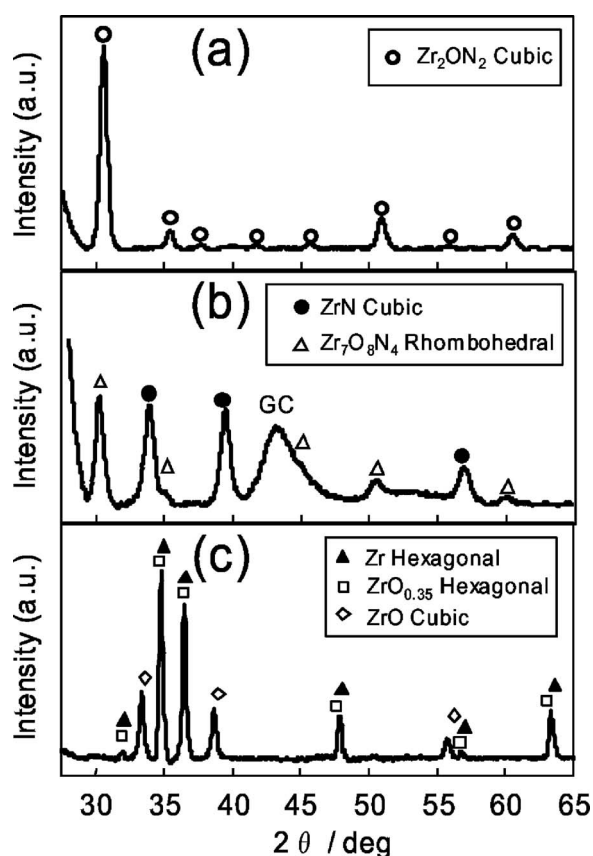


**Figure 4.** Thin-film XRD patterns of  $\text{ZrO}_x\text{N}_y$  prepared at (a)  $p_{\text{N}_2}/p_{\text{O}_2} = 240$ , (b)  $p_{\text{N}_2}/p_{\text{O}_2} = 2400$ , and (c)  $p_{\text{N}_2}/p_{\text{O}_2} = 0$ .

therefore, the O content was a little larger than that of the theoretical value. Both the thin-film XRD and RBS analyses supported the formation of  $\text{Zr}_2\text{ON}_2$  in the thin film with a high catalytic activity.

Figure 5 shows the slow scan cyclic voltammograms (SSCVs) in the steady state of the  $\text{ZrO}_x\text{N}_y$  films prepared at conditions corresponding to Fig. 2a-c under a  $\text{N}_2$  atmosphere. The SSCV of  $\text{ZrO}_x\text{N}_y$ , which was prepared at  $p_{\text{N}_2}/p_{\text{O}_2} = 240$ , had no specific peaks. In addition, the anodic electric charge was almost equal to the cathodic one. These results indicated that the  $\text{ZrO}_x\text{N}_y$  with  $\text{Zr}_2\text{ON}_2$  structures

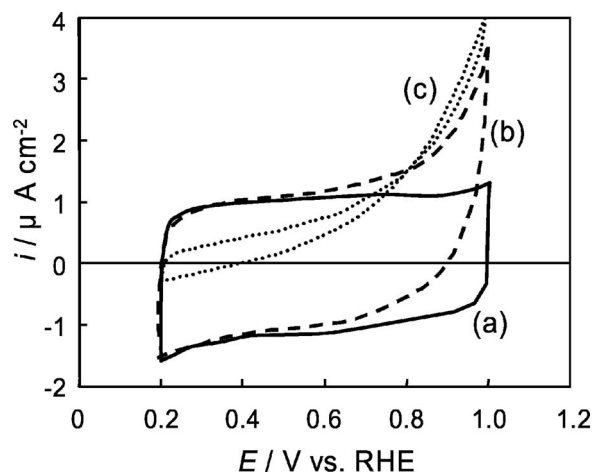


**Figure 5.** Steady-state SSCVs of  $\text{ZrO}_x\text{N}_y$  under a  $\text{N}_2$  atmosphere in 0.1 M  $\text{H}_2\text{SO}_4$  at 30°C with a scan rate of 5  $\text{mV s}^{-1}$ : (a)  $p_{\text{N}_2}/p_{\text{O}_2} = 240$ , (b)  $p_{\text{N}_2}/p_{\text{O}_2} = 2400$ , and (c)  $p_{\text{N}_2}/p_{\text{O}_2} = 0$ .

had high electrochemical stability in 0.1 M  $\text{H}_2\text{SO}_4$  at 30°C. Large anodic currents were observed at the SSCV of  $\text{ZrO}_x\text{N}_y$  prepared at  $p_{\text{N}_2}/p_{\text{O}_2} = 2400$  ( $\text{ZrN}$  and  $\text{Zr}_7\text{O}_8\text{N}_4$  by thin-film XRD) and  $\text{ZrO}_x\text{N}_y$  prepared at  $p_{\text{N}_2}/p_{\text{O}_2} = 0$  (metallic Zr and zirconium oxides with low oxidation state of Zr by thin-film XRD). In particular, the metallic Zr,  $\text{ZrO}$ , and  $\text{ZrO}_{0.35}$  were unstable in acid solution because the anodic current was observed even at the cathodic potential scan. Zirconium nitrides, Zr,  $\text{ZrO}$ , and  $\text{ZrO}_{0.35}$ , had poor electrochemical stabilities.

Both an adsorption of oxygen molecules and a desorption of water molecules are required to continue the ORR smoothly. When the oxidation state of Zr in the catalyst was close to the metallic state, that is, the Zr had a lower oxidation number, the interaction between Zr and oxygen was so strong that the oxygen stuck on the surface strongly and the desorption of the water molecules barely occurred. When the Zr had a higher oxidation number, the interaction was too weak for the adsorption of the  $\text{O}_2$  molecules to proceed. Therefore, an intermediate oxidation number of Zr in the catalyst was suitable for the moderate interaction between the Zr and oxygen, and the ORR proceeded smoothly on the active site.

Mishima et al. have investigated the  $\text{Zr}_2\text{ON}_2$  as a visible-light photocatalyst.<sup>8</sup> The bandgap of  $\text{Zr}_2\text{ON}_2$  was 2.6 eV. Although the upper energy level of the electron in the valence band of  $\text{Zr}_2\text{ON}_2$  was unknown, it was lower than  $-5.6$  eV, because no oxygen gas evolved when the upper energy level was higher than  $-5.6$  eV. That is, the ionization potential of the  $\text{Zr}_2\text{ON}_2$  was expected to be higher than 5.6 eV. We measured the ionization potential of the  $\text{ZrO}_x\text{N}_y$  with  $\text{Zr}_2\text{ON}_2$  structure using a photoelectron spectroscopic analyzer to estimate the electronic structure of the specimen. The ionization potential of the  $\text{ZrO}_x\text{N}_y$  with a  $\text{Zr}_2\text{ON}_2$  structure was determined to be 5.06 eV. This value was lower than that expected on the  $\text{Zr}_2\text{ON}_2$ , 5.6 eV. In general, the ionization potential of the oxides decreases with an increase in the surface defect density.<sup>9-12</sup> The low ionization potential of the  $\text{ZrO}_x\text{N}_y$  suggested that although the  $\text{ZrO}_x\text{N}_y$  prepared using reactive sputtering had the  $\text{Zr}_2\text{ON}_2$  structure, it had some surface defects which created the donor levels close to the edge level of the conduction band, that is, close to the Fermi level. The electrons in the donor level due to the surface defects probably participate in the ORR, although the structure of the defect was not clear.

## Conclusions

We investigated the dependence of the catalytic activity of  $\text{ZrO}_x\text{N}_y$  prepared by reactive sputtering for the ORR on the gas atmosphere during film formation at a substrate temperature of 800°C. The  $\text{ZrO}_x\text{N}_y$  prepared at  $p_{\text{Ar}} = 0.886$  Pa,  $p_{\text{N}_2} = 0.41$  Pa, and  $p_{\text{O}_2} = 1.7$  mPa had the highest catalytic activity, and the onset potential for the ORR was ca. 0.8 V vs RHE. The thin-film XRD analysis revealed that the  $\text{ZrO}_x\text{N}_y$  with the highest catalytic activity for the ORR had a  $\text{Zr}_2\text{ON}_2$  crystalline structure. However, the ionization potential of  $\text{ZrO}_x\text{N}_y$  with a  $\text{Zr}_2\text{ON}_2$  structure was 5.06 eV, which was lower than the expected value of  $\text{Zr}_2\text{ON}_2$  ( $>5.6$  eV). This result indicates that the  $\text{Zr}_2\text{ON}_2$  structure with some surface defects could be very important toward production of a highly active catalyst for ORR.

## Acknowledgments

The authors thank the New Energy Industrial and Technology Development Organization (NEDO) for financial support. In addition, the authors thank Dr. T. Yokoyama for his kind assistance with the analysis of the crystalline structure and Riken Keiki Co., Ltd. for their ionization potential measurements.

Yokohama National University assisted in meeting the publication costs of this article.

## References

1. T. Toda, H. Igarashi, H. Uchida, and M. Watanabe, *J. Electrochem. Soc.*, **146**, 3750 (1999).

2. S. Mukerjee, S. Srinivasan, M. P. Soriaga, and J. McBreen, *J. Phys. Chem.*, **99**, 4577 (1995).
3. K. Yasuda, A. Taniguchi, T. Akita, T. Ioroi, and Z. Siroma, *J. Electrochem. Soc.*, **153**, A1599 (2006).
4. S. Doi, A. Ishihara, S. Mitsushima, N. Kamiya, and K. Ota, *J. Electrochem. Soc.*, **154**, B362 (2007).
5. A. Ishihara, K. Lee, S. Doi, S. Mitsushima, N. Kamiya, M. Hara, K. Domen, K. Fukuda, and K. Ota, *Electrochem. Solid-State Lett.*, **8**, A201 (2005).
6. Y. Shibata, A. Ishihara, S. Mitsushima, N. Kamiya, and K. Ota, *Electrochem. Solid-State Lett.*, **10**, B43 (2007).
7. G. Liu, H. M. Zhang, M. R. Wang, H. X. Zhong, and J. Chen, *J. Power Sources*, **172**, 503 (2007).
8. T. Mishima, M. Matsuda, and M. Miyake, *Appl. Catal., A*, **324**, 77 (2007).
9. U. Vohrer, H.-D. Wiemhöfer, W. Göpal, B. A. Van Hassel, and A. J. Burggraaf, *Solid State Ionics*, **59**, 141 (1993).
10. W.-J. Chun, A. Ishikawa, H. Fujisawa, T. Tanaka, J. N. Kondo, M. Hara, M. Kawai, Y. Matsumoto, and K. Domen, *J. Phys. Chem. B*, **107**, 1798 (2003).
11. H. Gerisher, *Z. Phys. Chem., Neue Folge*, **26**, 325 (1960).
12. V. E. Henrich, G. Dresselhaus, and H. J. Zeiger, *Phys. Rev. Lett.*, **36**, 1335 (1976).